The results of a programme to evaluate the measurement of the critical current of relatively small (<600 A) practical superconductors are presented. Experimental data showing the effect of various parameters on the measurement are given. Specific areas covered are: experimental design and sample mounting; electric field and resistivity criteria; temporal and spatial variations in the field and current; and temperature and strain effects. The goal of the presentation is to describe the critical current measurement process and its pitfalls in sufficient detail to serve as a guide for those relatively new to the field of practical superconductors.

Critical current measurements: a compendium of experimental results

L.F. Goodrich and F.R. Fickett

Key words: superconductor, critical current, data

Accurate measurement of the critical current, I_c, of practical superconductors is a subject of concern both technically and in the commerce associated with these materials. The measurement is not a simple one and it is not unusual to find that two critical current determinations for the same material disagree by large amounts, often of the order of 20-30%. In an attempt to explain the source of some of these discrepancies and to promote more uniform measurements, a cooperative standards programme involving DoE, NBS, and ASTM was begun. Research was undertaken at NBS and by the US wire manufacturers that would ultimately lead to an ASTM Standard for the measurement of critical currents below 600 A. The results of the programme to date have been published[1,2] and a draft standard is now being evaluated by the ASTM membership. In the course of the programme many measurements were made at NBS to evaluate the effect of various experimental parameters on the critical current determination. In this paper we present the results of these measurements and discuss their effect on the measured critical current.

Our objective here is to present adequate information so that a technically knowledgeable person can make an accurate measurement of the critical current of a commercial superconductor. This task involves the construction of a proper apparatus and the use of a correct measurement technique. The effect of the most important parameters (eg field orientation) on the results are treated in detail in separate sections; usually with data showing the result of variations in the parameter on the measurement.

We deal here only with practical superconductors, usually multifilamentary niobium-titanium (NbTi) or niobium-tin (Nb_3Sn) wire with a copper matrix, although Nb_3Sn tape conductor is mentioned occasionally. The general construction is shown in Fig. 1 and a cross section of a complex conductor in Fig. 2. Most practical conductors are not round (and sometimes not monolithic) and this leads to a whole new set of field orientation effects. Most of what we have to say will, of course, apply to any superconductor, but some of the topics (eg matching of thermal contraction) will require re-evaluation for conductors of significantly different composition from those investigated here. Also it is important to realize that commercial superconductors are subject to significant variability in their properties due to variations both in basic materials and in processing from one wire lot to the next.[2] Thus, frequent measurements of the critical current are required in order to maintain quality control and the measurement technique should reflect this by being as easy as possible to use.

The basic data from which the critical current of a practical superconductor is determined is a plot of voltage, V, as a function of current, I: the V-I characteristic. It is assumed that other parameters such as applied field, temperature, strain, and displacement are constant during this measurement. A typical real V-I characteristic is shown in Fig. 3. The curve should be reversible (taking into account any dI/dt voltage); irreversibility is an indication of potential problems such as sample heating. The most common types of sample holders and magnets are shown schematically in Fig. 4, the reasons for choosing one configuration over another will be discussed later. The V-I characteristic of Fig. 3 shows one problem immediately: a unique critical-current value is difficult to define here. This problem is resolved pragmatically by the selection of a critical current criterion, either a specific value of electric field, E_c (voltage per unit length), measured along the wire or an effective resistivity (a line of some specific slope, E/J, in $\Omega \cdot$ cm where J is the current density). The philosophy of the curve selection process and its effect on the results will be discussed at length. Further problems arise in that the low current part of the curve in Fig. 3 is actually showing a phenomena, known as current transfer, that is determined by the sample mounting and/or measurement configuration and is not intrinsic to the wire. It arises as currents flow through the resistive matrix between superconducting filaments in response to changing conditions. Its presence does not necessarily degrade the accuracy of the measurement, but it may. The high current portion of the curve does represent an intrinsic property of the superconductor, the flux flow voltage, that arises from the motion of flux vortices across the superconductor. There is an empirical relationship that shows the voltage in this region to be proportional to some power of the current, more about that later.

The authors are at the Electromagnetic Technology Division, National Bureau of Standards, Boulder, Colorado 80303, USA.
Paper received 6 January 1982. The work was supported in part by Department of Energy, Division of High Energy Physics, Office of Fusion Energy, and Magnetohydrodynamics Division through Massachusetts Institute of Technology.

0011-2275/82/005225-17 $03.00

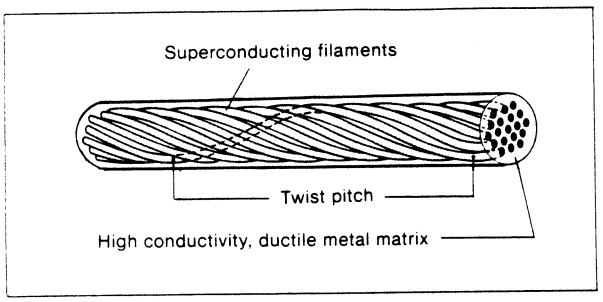

Fig. 1 Construction of a simple twisted multifilamentary superconductor. Typical of NbTi composite

Another aspect of practical conductors that needs mentioning is their stability, the amount of disturbance, either mechanical or thermal, that the conductor will tolerate before thermal runaway (or quench) occurs. This property is controlled by the addition of relatively pure metal, most often copper, to the conductor composite. More copper results in greater stability, but a lowered overall current density for the conductor which is frequently undesirable in magnets. Superconductor stability is a complex topic, but one that has been frequently discussed in the literature.[3] The degree of stability of a wire should not greatly affect the measured critical current, but the actual experiment is more difficult to perform on marginally stabilized wires.

The rest of the paper is divided into five major sections covering: the design of our apparatus, the choice of materials for the test programme, a discussion on the effect of various parameters on the design of critical current experiments, and the experimental measurements and their interpretation. The results are summarized in the final section.

Apparatus

There is an important distinction to be made immediately. In this section we describe our apparatus constructed for the rather complex and sensitive experiments needed to evaluate various aspects of critical current measurement. In later sections we will be discussing the design of experimental systems that may well be less complex than ours. In general, we feel that any system that takes into account the applicable constraints of the later sections will be adequate for critical current measurements with an inaccuracy of ±5%.

A schematic diagram of our apparatus is shown in Fig. 5. Each of the parts is discussed in more detail below. Regardless of the specific configuration chosen, the system will measure the appropriate critical current to better than ±5% and reproduce a given measurement to better than 0.5%.

Sample holders. Sample holders of each of the types shown in Fig. 4 were constructed, since one of our goals was to determine the limits of useful application for each type. In addition, numerous holders representing modifications of these were made for specific tests. Some examples are: coils with variable turns-per-centimeter to evaluate field angle effects and a rotating table system for the same purpose; flat bottom hairpin holder to evaluate the effect of small radius of curvature; various configurations of the short straight current leads, used in studying current injection effects; and holders that allow placement of voltage taps on opposite sides of the sample while still maintaining support against the Lorentz force. In each holder, except those designed to measure orientation effects, the applied magnetic field is essentially perpendicular to the sample axis, at least between the voltage taps. This is the orientation in which the minimum critical current will be measured and, thus, represents the limiting case for most applications.

Nearly all of the holders are made from fibreglass-epoxy matched to the sample for relative thermal contraction as discussed below. Several of them are shown in Fig. 6. High current NbTi bus bar (>700 A at 8 T) was used for the current contacts. These were epoxied into grooves in the sample holder with a high temperature version of a commercial filled epoxy. This technique allows repeated soldering of samples without loosening of the bus bar.

Sample voltage detection and current supply. As shown in Fig. 5, the sample voltage is read by an analogue nanovoltmeter and, after filtering, is plotted on the Y axis of an X-Y recorder (some early comparisons were made between this system and a digital multimeter with an analogue output). The input cord of the nanovoltmeter has copper clips that are manually clipped to the appropriate set of terminals on the wire bundle from the sample holder, which may contain as many as sixteen wires. This is the only junction between the sample and the nanovoltmeter input. Isothermal conditions were maintained by putting small bags of lead shot under and on top of the junction.

The sample power supply for most measurements was a series-regulated 600 A battery driven by a commercial ramp generator. For comparison studies and the evaluation of ripple and noise, a 600 A silicon-controlled rectifier (SCR) regulated supply was used. In each case standard current shunts (±0.25%) were used to measure the current and/or drive the Y axis of the recorder. Current leads into the dewar were commercial 600 A vapour-cooled leads.

The most sensitive of the possible configurations, the nanovoltmeter and battery power supply, allows the measurement of voltages as low as ten nanovolts. This is a much greater sensitivity than required for conventional critical

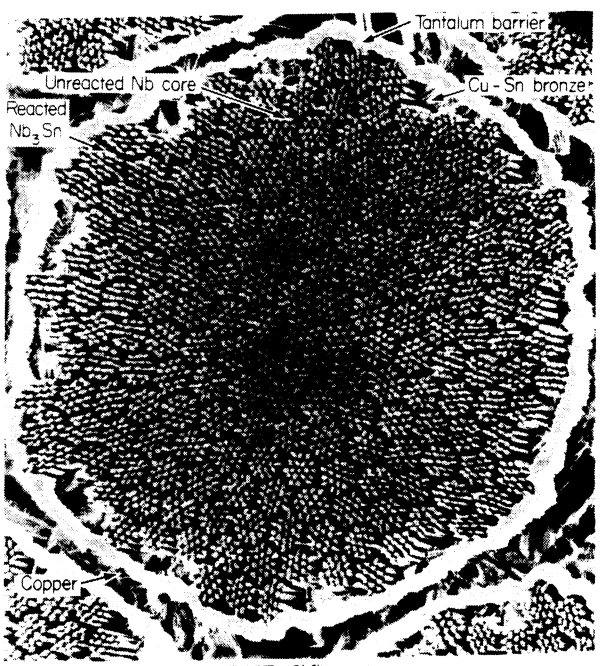

Fig. 2 A complex composite superconductor based on Nb_3Sn

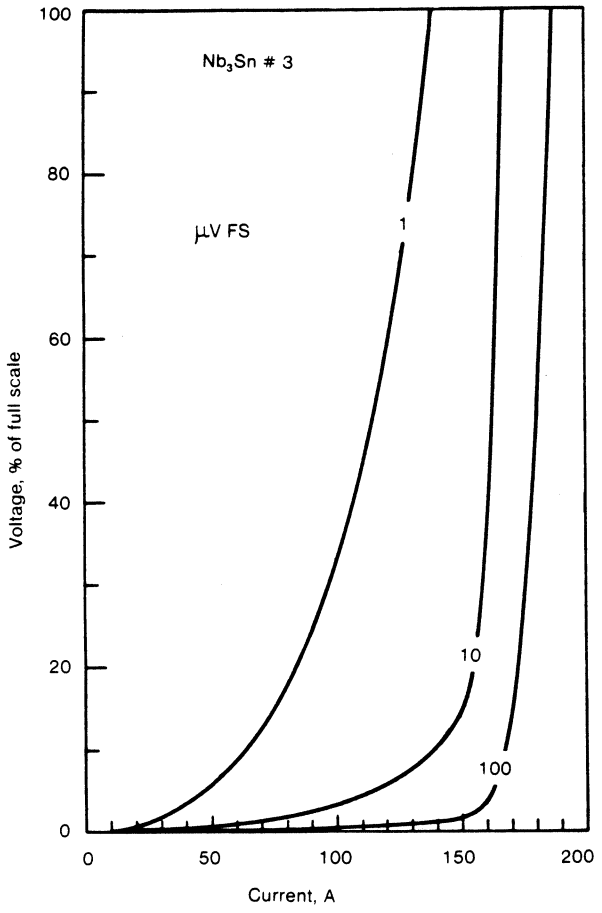

Fig. 3 Typical *V–I* characteristic for a commercial superconductor (multifilamentary Nb_3Sn at 7 T). The curves show the structure of the curve at different voltage detection levels

current measurements, with the possible exception of the evaluation of wire used in magnets for nuclear magnetic resonance (NMR) measurements.

The desire that the *V–I* curve be reversible for all measurements on all samples requires a quench-protect circuit. The circuit diagram of our quench protect (adopted from a Los Alamos National Laboratory design) is shown in Fig. 7. The voltage across the entire sample at the current bus bars is detected and used to shut down the current ramp. The level at which this shutdown occurs is adjustable by means of a front-panel dial. This circuit is not absolutely necessary. Especially in the case where many measurements are to be made on similar wires an experienced operator can easily prevent thermal runaway after a few samples have been quenched.

Magnet systems. Both types of magnets shown in Fig. 4 were used in these experiments. The simple solenoid was a 10 T magnet with a 3.8 cm bore. The split-pair magnet used for the long straight configuration measurement had a maximum field of 7 T and a radial access port of 1.5 cm (5 cm bore). Both magnets have been calibrated to a field accuracy of ±0.2% and a reproducibility of ±0.1%. At very low fields trapped flux could degrade these numbers significantly, but none of the measurements reported here involve that field region.

Materials

As mentioned earlier, one of the goals of the research described here was to develop supporting data for a standard test method for general laboratory use in the measurement of critical current. In this endeavour we limited our consideration to commercial superconductors with high field critical currents less than about 600 A, since this represents a practical limit for many laboratories. The materials used for our tests are described in Table 1. Sample numbers in the text and figures refer to this table.

The first wire listed in the table is one that has been used for numerous experiments at NBS over the years. The second wire is similar to the first except it is round. This wire was added to the group when the effect of the aspect ratio of rectangular wires discussed below was observed. The multifilamentary Nb_3Sn is a conventional wire that we react after forming; note that the filaments are untwisted. The lack of a twist pitch helps considerably in understanding the intricacies of current transfer along and across the wire as discussed below. The tape conductor is most helpful as a 'worst case' sample in the evaluation of field orientation and current ripple effects.

Many lengths of each of these conductors were used throughout the tests reported here. Thus, as already mentioned, some sample-to-sample variation in properties is to be expected. Our experience indicates that, with careful sample selection, this should not result in more than about a 2% variation in critical current among samples of a given material as used here. This source of uncertainty could be minimized by use of a carefully characterized standard reference material and this possibility is now being explored at NBS.

Experiment design

This section and the following one present the bulk of our data on the various factors that influence the correct determination of critical current. In each instance we discuss the implications of the data for the design and operation of an

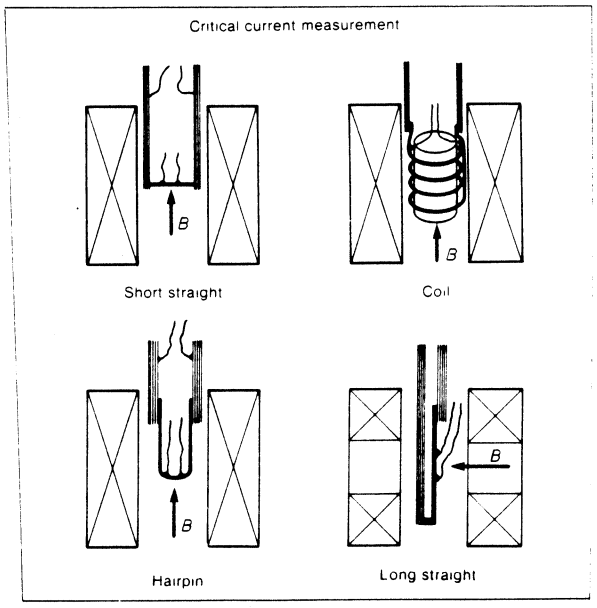

Fig. 4 Common sample holders and configurations used for critical current determination

Table 1. Critical current test materials

Sample number	Type	Dimensions, mm	Number of filaments	Twist, cm^{-1}	Copper to non-copper ratio	Approximate critical current at 8 T, 4 K, A
1	Rectangular NbTi	0.53 x 0.68	180	0.79	1.8	114
2	Round NbTi	0.64	180	0.79	1.8	128
3	Round Nb_3Sn	0.70	2869	0	1.7	132
4	Tape Nb_3Sn	0.2 x 2.3	–	–	1.6	172

experimental apparatus. The general details of cryogenic apparatus construction are not treated here, but excellent texts on the subject are available.[4]

In this section we present data related to the design and construction of the experimental apparatus. It is probably possible to construct a perfect apparatus for the determination of I_c, but the restrictions of the real world make this attainment unlikely. Most of us must take into account the limitations of space, existing equipment, time, and money. With this in mind, we have tried to present a design philosophy that allows choices to accommodate such restrictions while still maintaining the overall measurement accuracy. At the least, we hope that the data presented will indicate the consequences of various design choices.

Sample holders. The major sample holder types are shown in Fig. 4. Table 2 gives a comparison of the various types. The terms used have already been introduced, but they will also be discussed in detail below. It should be stressed that, in some circumstances, the effects listed as disadvantages may, in fact, preclude the use of that holder for measurements on a specific material. In all cases the sample should be fit closely to the holder to avoid buckling in the field, this is especially important for the coil geometry. The use of small amounts of varnish or grease to hold the sample in place is usually acceptable, but see the comments below on heating.

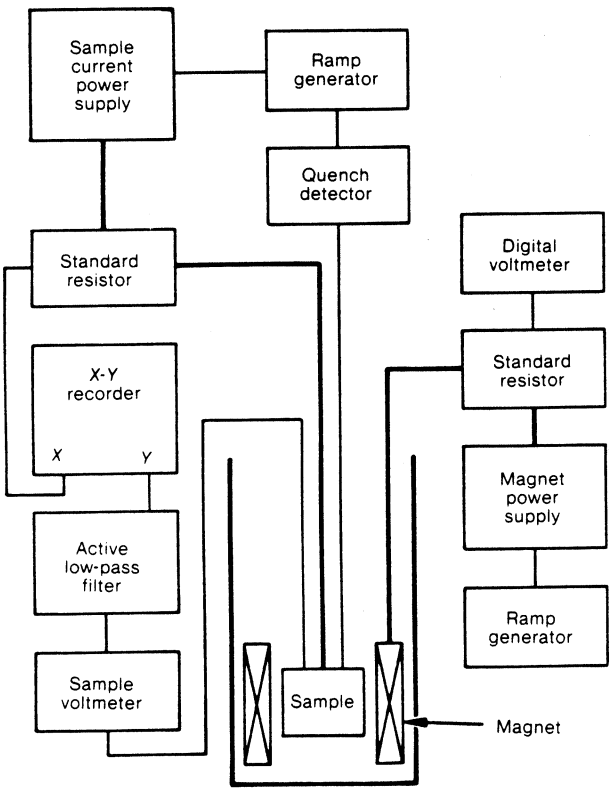

Fig. 5 Electrical systems for critical current measurement

Typical V-I data taken with the various holders are shown in Fig. 8. The plot is made on a full-log grid to illustrate that the curve usually has two regions that must be considered. The high current behaviour is representative of flux flow and is intrinsic to the superconductor. The data in the lower current region illustrate the varying role of current transfer in each design. This current transfer voltage must be subtracted in some manner in order to arrive at the intrinsic V-I curve from which I_c is determined. It is obvious from the figure that this problem becomes more acute as the electric field criterion decreases. Table 3 and Fig. 9 illustrate how the critical current determination at various fields and criteria is affected by sample holder type. A current transfer correction has been made to these data. Notice (see Fig. 8 and Table 3b) that, when the current transfer voltage is the same size or larger than the criterion used, the possibility exists of over- or under-estimating the current transfer part which may lead to large errors.

Clearly the choice of a sample holder requires some serious thought. Similarly, many of the problems vanish when a proper choice is made. It should be noted that most data presented here are for Nb_3Sn; the situation is generally much less severe for NbTi, as shown in Table 3, because the current transfer voltage is generally lower. However, at very low criteria ($\sim$10 nV cm^{-1}), the possibility of error from this source must be considered as can be seen in the table.

Voltage and current. The two problems to be resolved with regard to voltage and current leads are: how to get current into the sample and properly distributed among the superconducting filaments in as short a distance as possible; and, how to arrange the voltage taps so as to make the most meaningful measurement. Both of these problems are far more complex with a multifilamentary superconductor

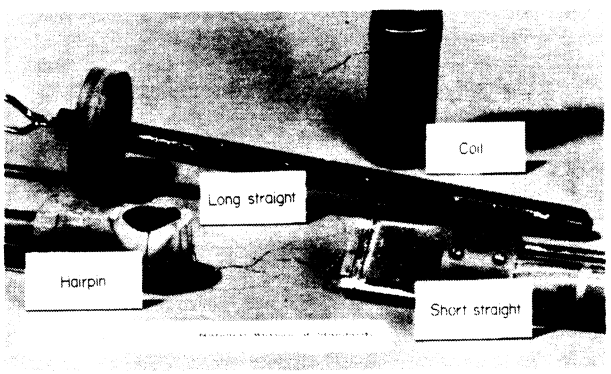

Fig. 6 Actual sample holders of the types shown in the drawing of Fig. 4

composite than they would be with, say, a simple copper wire. Again, the complexity is greater for the Nb_3Sn conductors.

The large sample currents used in these tests are usually brought into the cryostat by means of commercial helium-vapour-cooled leads. Current is monitored by a conventional, low-resistance, series shunt at room temperature. In the cryostat, the leads connect to a superconducting current bus of much higher capacity than the samples (I_c at least double). Monolithic rectangular NbTi conductor is handy for this purpose unless flexible leads are needed, in which case a bundle of smaller wires is appropriate. In most geometries, an added measure of protection is achieved because the current bus is parallel to the magnetic field in the high field region.

Transfer of the current from the bus into the sample is a complex process involving: the length and resistance of the joint;[5] the size, distribution, and twist pitch of the sample filaments;[6] and the details of current transfer between the filaments of the sample.[7] Large voltages can arise due to these mechanisms that may overwhelm the intrinsic V-I data. In the papers cited, a large amount of data is presented on each of these topics. It can be summarized by saying that a perfectly adequate situation will be achieved if the current contact length is at least ten times the maximum transverse dimension of the sample. For conductors with twisted filaments this contact length should also be greater than one twist pitch. These requirements are easily met for all sample configurations except the short straight. There it is usually possible to bend the sample into a 'flat-bottom hairpin' shape (or, in the case of multi-filamentary Nb_3Sn, to react to this shape) such that a reasonable length lies along the bus bars. This approach helps to an extent.[6] It is important that none of the free wire between the bus bars be bent, ie, the entire bend region should be soldered to the bar (except for a multi-filamentary Nb_3Sn sample that has been reacted to this shape or if the bend of a NbTi sample is not too severe).

Table 2. Sample holder comparisons

Sample geometry	Advantages	Disadvantages
Short straight	simple geometry solenoidal magnet	high contact heating high current transfer insensitive criteria
Long straight	low contact heating moderate criteria simple geometry	some current transfer split-pair magnet
Hairpin	low contact heating moderate criteria solenoidal magnet	some current transfer moderate geometry
Coil	low contact heating low current transfer sensitive criteria solenoidal magnet	complicated geometry

Even with reasonable current contact lengths, if the voltage taps are too close to the contact, large voltages related to the current transfer may be seen. The situation is significantly worse when marginal current contact lengths are used. The data shown in Fig. 10, taken on a coil sample of our Nb_3Sn wire illustrate all of the above points. These data were obtained by making a set of measurements of the voltage between adjacent taps on the sample and then cutting the sample in the current contact region and repeating the measurements. The value used for the distance, x, of the pair of voltage taps from the current contact was obtained by an iterative process that takes into account the

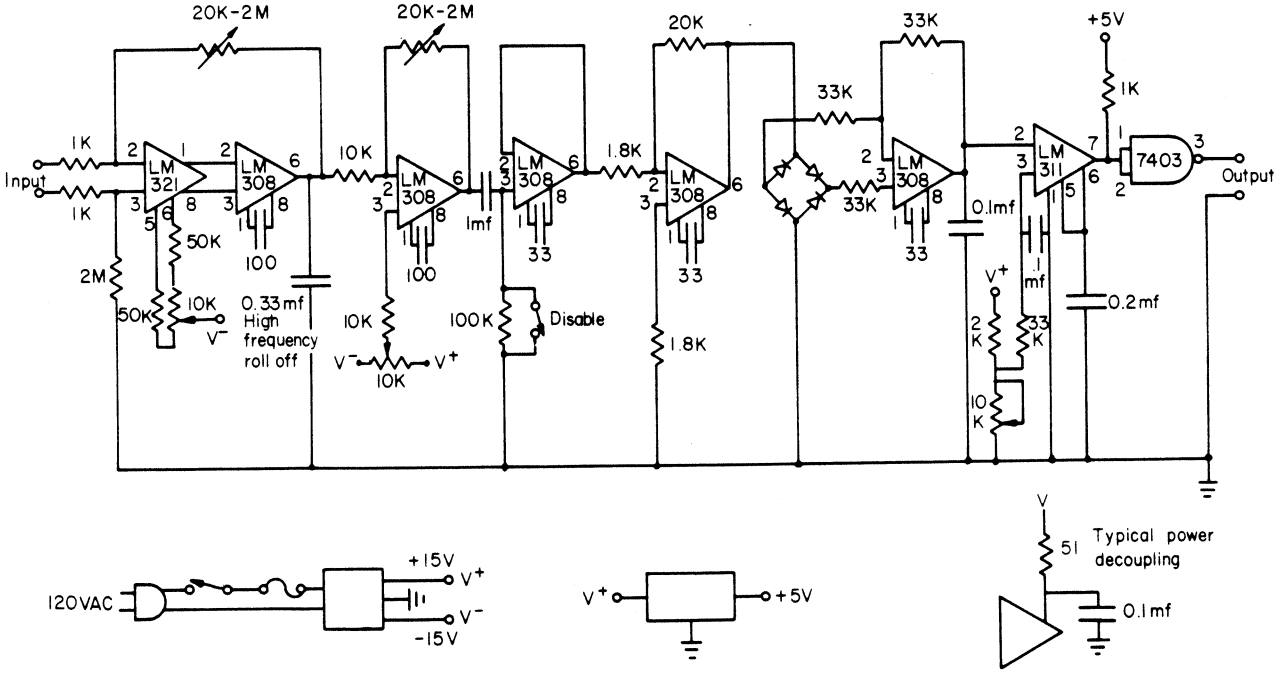

Fig. 7 Circuit diagram for a quench protection system. The resistors are marked with units of ohms and the capacitors with units of picofarads unless otherwise noted

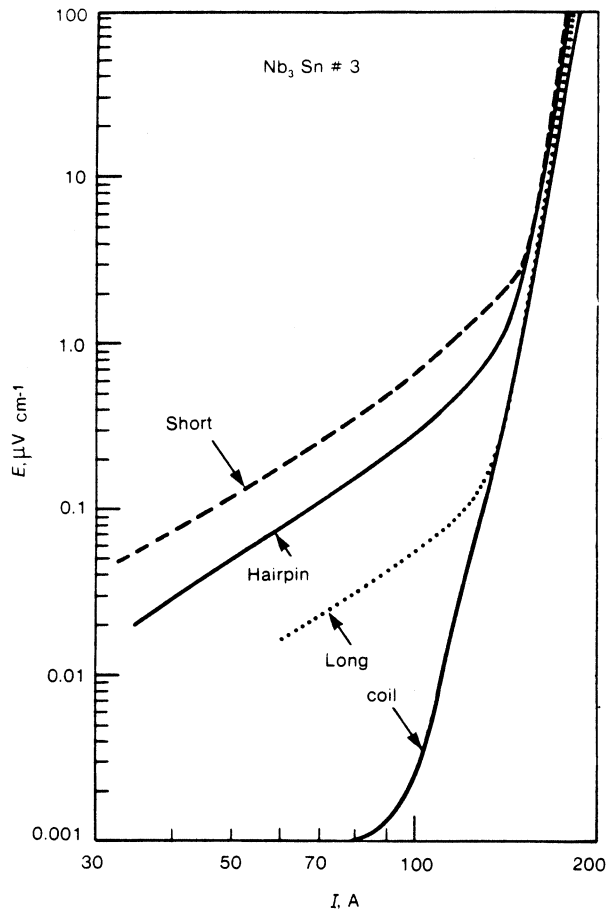

Fig. 8 Full log plot of representative *I–V* characteristics (multifilamentary Nb_3Sn at 7 T) for different sample holders

electric field as a function of position. The points on the plot at the largest x were taken on voltage taps positioned around the centre of the coil sample. In general the data indicate that length of free sample contact on the bus bar is not as effective in minimizing these voltages as is length of beyond the contact before the first voltage tap.

The behaviour illustrated by the data in Fig. 10 represents a complex aspect of practical superconductors that has been the subject of much study. A rule of thumb which will keep the current transfer voltages small in any arbitrary conductor is to make the free length between the current contact and the first voltage tap greater than the conductor's current transfer length,[7]

$$L = (0.1/n)^{1/2} (\rho_m/\rho^*)^{1/2} d \qquad (1)$$

Here ρ_m is the resistivity of the interfilament material, d the diameter of the filament region, n characterizes the sharpness of the superconductor's resistive transition (see below), and ρ^* is the resistivity equivalent to the criterion used to determine the critical current. For critical current measurements at a ρ^* of 10^{-11} Ω•cm, a free length 30 times the transverse dimension d will typically be more than adequate for Nb_3Sn:bronze conductors. The required length becomes greater as the critical-current criterion becomes more sensitive, however. Once again, the problems are minimal with NbTi:copper where the required length is typically 15 to 20 times less than for Nb_3Sn:bronze conductor. These general requirements on the free sample length are conservative. Free lengths shorter than the expression for L may well do the job, especially if the current contact is long, as shown in Fig. 10. Measurements made at low voltage levels may give strange results (including negative voltages) in the case of very short current injection contacts.[6]

Another aspect of the current transfer problem is that the redistribution of current among the filaments can occur near a change in magnitude or angle of the applied magnetic field as well as adjacent to a joint. This was observed in obtaining the data shown in Fig. 8. The long geometry is an example of the sample in a field gradient. The total length of sample #3 (Nb_3Sn) measured in this geometry was 22 cm (550 d), which put the ends of the sample in a very low field region (5 cm bore). A number of voltage taps were placed along the sample and a current transfer voltage was observed adjacent to the joint and in the bore region, however, there was a region (a few centimetres long) in between these two where the current transfer electric field was very small (less than a few nV cm^{-1}) even up to the I_c of the bore region. A profile of the current transfer electric field in the field gradient region indicated gradual increase of E with increasing field through this region, then a slight decrease in the bore region. This same kind of separation of these two causes was also observed in the hairpin sample where instead of a field gradient region there is a change in angle between the sample and the magnetic field. Both of these

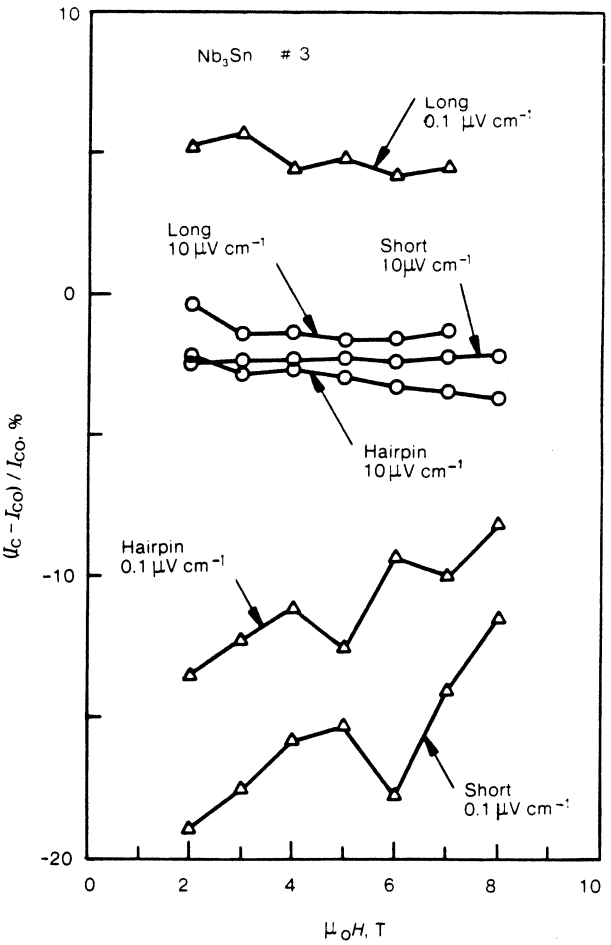

Fig. 9 The percentage change in I_c observed for a Nb_3Sn sample (# 3) with different sample holders as a function of magnetic field. The base data that defines zero is that from the coil sample, I_{co}. Results are shown for two values of the electric field criterion

Table 3a. Comparisons of critical current data for various sample geometries as a function of magnetic field and criterion for a NbTi conductor (Entries give percent difference with respect to the coil I_c)

	Field, T	2	3	4	5	6	7	8	9
$E_c = 1\,\mu V\,cm^{-1}$	Coil, I_c	455.2	350.7	284.6	234.3	190.4	150.4	111.3	72.3
	Long	–	-1.3	-1.1	-0.8	-0.6	-0.3	–	–
	Hairpin	0.6	0.5	0.6	0.6	1.0	1.0	1.4	–
	Short	0.3	0.6	0.7	0.8	1.4	1.5	2.1	2.3
$E_c = 0.1\,\mu V\,cm^{-1}$	Coil, I_c	431.5	332.0	269.2	221.4	179.8	141.8	104.6	67.0
	Long	–	-1.4	-1.3	-1.0	-0.6	-0.4	–	–
	Hairpin	1.3	1.2	1.4	1.4	1.8	1.7	1.9	–
	Short	0.3	0.8	0.9	1.1	1.5	1.5	2.1	2.5
$E_c = 0.01\,\mu V\,cm^{-1}$	Coil, I_c	411.1	315.7	255.4	210.5	170.6	134.0	98.2	62.2
	Long	–	-2.6	-2.7	-1.9	-0.6	-0.3	–	–
	Hairpin	0.2	2.0	3.0	0.7	1.4	2.2	-0.2	–
	Short	-2.2	0.6	1.3	0.8	2.1	2.9	2.7	4.4

Table 3b. Comparison of critical current data for various sample geometries as a function of magnetic field and criterion for a Nb_3Sn conductor (Entries give percent difference with respect to the coil I_c)

	Field, T	2	3	4	5	6	7	8
$E_c = 10\,\mu V\,cm^{-1}$	Coil, I_c	539.1	397.4	307.9	247.3	202.9	167.4	139.4
	Long	-0.4	-1.4	-1.4	-1.6	-1.6	-1.3	–
	Hairpin	-2.2	-2.9	-2.7	-2.9	-3.3	-3.5	-3.7
	Short	-2.5	-2.4	-2.3	-2.3	-2.4	-2.3	-2.2
$E_c = 1\,\mu V\,cm^{-1}$	Coil, I_c	480.4	354.8	275.5	221.4	181.4	149.7	124.6
	Long	2.2	0.7	0.3	0.0	-0.2	0.1	–
	Hairpin	-2.8	-2.3	-1.9	-2.4	-2.6	-2.9	-3.2
	Short	-10.7	-8.4	-6.2	-4.4	-4.7	-2.7	-1.3
$E_c = 0.1\,\mu V\,cm^{-1}$	Coil, I_c	416.8	308.8	239.3	191.8	156.8	129.5	107.6
	Long	5.2	5.6	4.4	4.8	4.2	4.5	–
	Hairpin	-13.5	-12.3	11.1	-12.5	-9.3	-10.0	-8.1
	Short	-18.9	-17.5	-15.8	-15.3	-17.7	-14.0	-11.5

observations indicate that no matter how long the low or parallel field region is, there can be a current transfer voltage in a temporal or spatial field variation and in fact the high perpendicular field region is necessary to complete the distribution of the current among the filaments. This is another advantage that the flat-bottom hairpin has over the curved bottom hairpin. In all cases the removal of the current transfer voltage adjacent to the joints from the measurement region is advantageous. The rule of thumb result given above is still valid; however, its application to these aspects of current transfer is more complex because of their distributed nature.

Protection of the sample against burnout during a quench has already been discussed and a quench-protect circuit is shown in Fig. 7. When many samples with highly resistive matrix materials (CuNi is sometimes used) must be measured, a reasonable alternative or adjunct to such a

Table 4. Values for n of the test sample

	NbTi rectangular sample #1			NbTi round sample #2		Nb_3Sn MF sample #3			Nb_3Sn tape sample #4		
Range of E, $\mu V\ cm^{-1}$	1.0	0.1	0.01	1.0	0.1	10	1.0	0.1	10	1.0	0.1
	0.1	0.01	.001	0.1	.01	1.0	0.1	0.01	1.0	0.1	.01
Field T											
2	43.0	47.7	43.5	55.4	84.2	20.0	16.2	17.4	73.1	150	279
3	42.1	45.3	31.8	57.2	80.2	20.3	16.6	16.4	71.4	173	261
4	41.3	45.2	34.2	56.7	75.0	20.7	16.4	16.5	72.4	162	208
5	40.6	46.8	41.6	53.7	68.7	20.8	16.0	15.6	70.0	151	191
6	40.4	45.9	39.1	50.7	61.8	20.6	15.8	15.4	65.4	143	184
7	39.1	43.2	36.3	45.5	53.5	20.6	15.9	14.4	59.4	126	166
8	36.9	37.5	31.2	36.8	43.3	20.5	15.6	13.4	52.4	109	150
9	30.0	30.9	27.0	27.1	31.4	20.4	15.3	12.4	45.1	89	107
9.5	25.0	24.2	24.5	–	–	20.2	15.0	12.0	41.0	82	96
10	19.1	18.5	19.4	–	–	20.0	15.0	11.4	–	–	–

circuit is the use of a resistive shunt in parallel with the sample, usually just soldered across the bus bars. The shunt, usually of copper with a residual resistivity ratio (rrr) ∿200, conducts very little of the current when the sample is superconducting and most of it when the sample is normal. In determining the actual current sharing between the sample and the shunt, the contact resistance of the various joints involved must be considered. It is not uncommon to solder the sample directly to the shunt. This practice is acceptable in most cases, but it should be realized that it can make an intrinsically unstable superconductor (ie, filaments too large, filaments not twisted enough, or not enough stabilizer) appear to be stable – a misleading result.

Voltage taps are usually soldered to the sample. Attachment to the bus bars is sometimes used for relatively crude measurements. Care should be taken to avoid creating stress concentration points. The measured voltage is most often used to calculate an electric field or resistivity which is then compared against a chosen criterion to define I_c. Proper use of these criteria requires attention to the concept of effective length. The problem is illustrated in Fig. 11. It arises when a part of the sample between the voltage taps is not in perpendicular field, a situation that is common for the hairpin geometry. As the sample approaches its critical current, the appropriate voltage develops on a-a. Dividing this voltage by the tap spacing, l_{aa}, gives the (nearly) correct electric field. However, if the voltage measurement is made on tap sets bb or cc a value nearly the same as that on aa will be seen because the sample lengths in a parallel field have not yet developed any voltage: they are not yet near to their critical current. Thus an electric field calculation using data from the cc taps and the measured distance between them along the wire would give a misleading result: a very low electric field. Thus, it is necessary to find an effective length that can be used in calculations. This can only be done by using a 'standard' wire that has been measured by some other technique.

The problem persists in a less drastic form all the way around the curve of a round-bottom hairpin sample because of the changing orientation of the wire with respect to the applied field. For example, a measurement made with probes located at opposite ends of a diameter on a round-bottom sample holder had a true effective length of 35% of the actual distance along the wire. Note that this length is even smaller than the perpendicular projected length. The basic conclusion is that the round-bottom hairpin geometry is not one to use if precise data are needed, but can be adequate for comparisons.

Magnetic field. Magnetic field is an expensive commodity and it is, thus, the parameter that usually determines the design details of the critical current measurement apparatus with regard to size and shape. Most high field laboratory

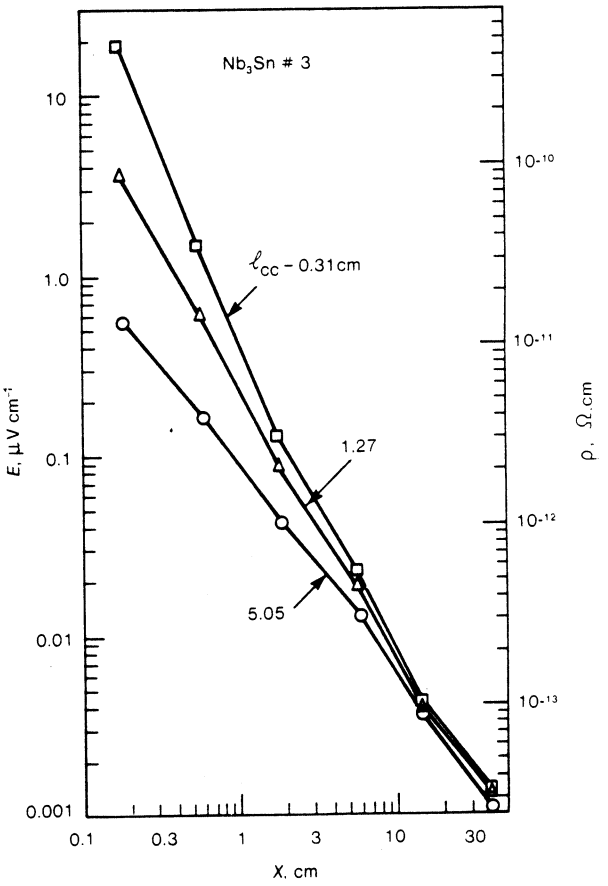

Fig. 10 Full log plot of the electric field (or effective resistivity) due to current transfer as measured at various distances, x, from the current contact. Each curve shows data for a different length current contact, l_{cc}, between the sample and the bus bar. The wire is multifilamentary Nb_3Sn measured at 4 T and 160 A (note the intrinsic I_c at 1 nV cm^{-1} is ∿186 A)

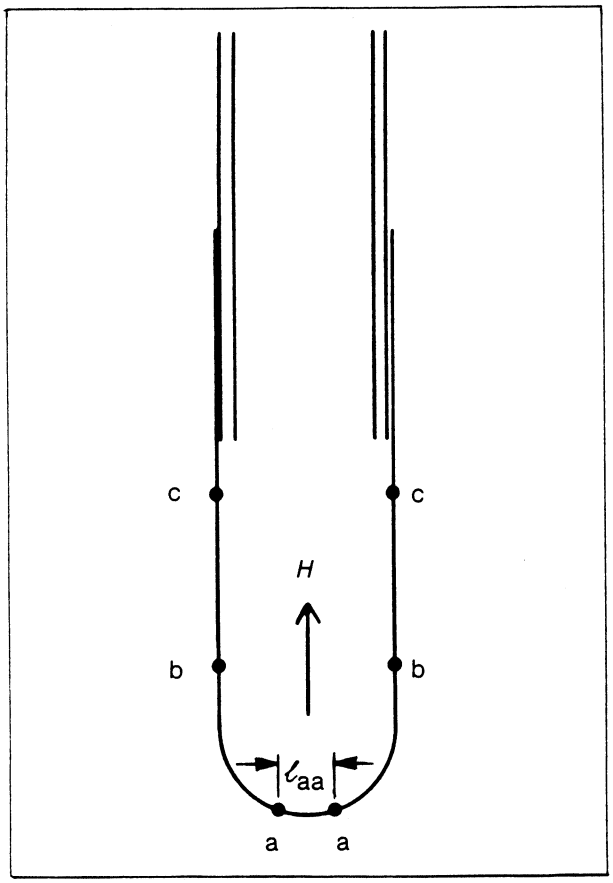

Fig. 11 Hairpin sample geometry to illustrate the concept of effective length (l_{aa} = length between taps a and a)

magnets are simple solenoids with bore diameters of <10 cm for 8 T NbTi magnets and <5 cm for 10 T Nb_3Sn/NbTi compound magnets. The region of 1% field homogeneity is usually of the order of a few centimetres.

The major design problem related to field configuration, once the size of things is fixed, is the angle between the conductor and the field. There are two aspects to this problem: one, the effect of a lack of perpendicularity between the sample axis and the field; and two, for rectangular conductors, the effect of the angle of an accurately perpendicular field with respect to, say, the wide face of the sample.

The first of these concerns was investigated in two ways. First, a series of coil samples were prepared with winding pitches varying from 1 to 40°. Total sample lengths varied from 10 to 90 cm. The results of the critical current measurements with these samples are shown by the open circles in Fig. 12. A more complete series of measurements were made on all samples using a rotating device that allows a single short (3.6 cm) sample to be rotated through a total angle of nearly 120° and the critical current measured at as many points as desired. These results are also shown in the figure. Two features are obvious: the sample can be misoriented quite considerably without seriously degrading the measurement accuracy (at least 8° before a 2% increase in I_c occurs); and, beyond a certain point the critical current increases very rapidly with field angle. The data for all samples presented here was taken in a field of 8 T, but data taken in 4 and 6 T had a very similar angular dependence when normalized to $(I_c - I_{co})/I_{co}$ (where I_{co} is the critical current with the field perpendicular to the sample axis) which suggests this magnetic field scaling for each sample. This magnetic field scaling was also observed for sample 2 (NbTi) at 9 and 9.75 T (note that I_{co} = 349 A at 4 T and I_{co} = 49 A at 9.75 T). Also, there was very little change in these curves over a wide range of critical current criteria for each of these samples. In addition, different types of NbTi conductor give similar behaviour. The behaviour of the multifilamentary Nb_3Sn is somewhat different, but the effect is similar to that for the Nb_3Sn tape. A twisted multifilamentary Nb_3Sn sample (prepared by twisting a length of sample 3 prior to its reaction) was also measured and its angular dependence of I_c was very similar to the untwisted sample. For each of the rectangular conductors, the field is parallel to the wide face during this measurement. If one attempts to explain the observed angular dependence, the first guess at the shape would be $I_c/I_{co} = 1/\cos\theta$ considering the perpendicular projection of the applied field. The NbTi I_c's increased faster with angle than this and the Nb_3Sn I_c's increased more slowly. Fig. 13 is a full log plot of the data showing the large angle (conductor and field closer to parallel) data as well. The leads to the rotating table device limited the measurement

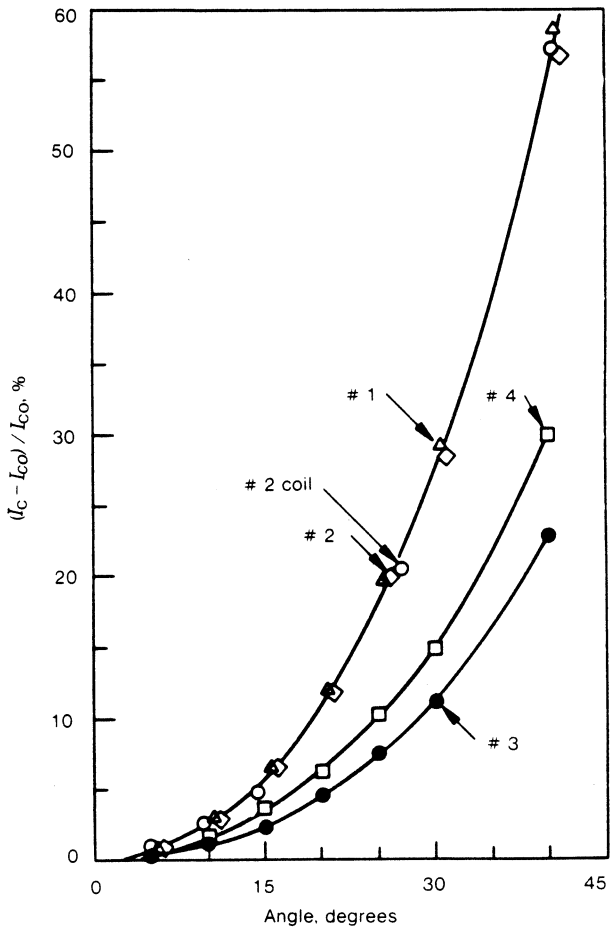

Fig. 12 The effect of the angle between the conductor axis and the applied field on the critical current determination. The angle is zero when the conductor axis is perpendicular to the applied field. I_{co} is the critical current at the zero angle. Data shown were taken with variable pitch coils (marked coil) and with a short-sample rotating table device. The numbered samples are described in Table 1

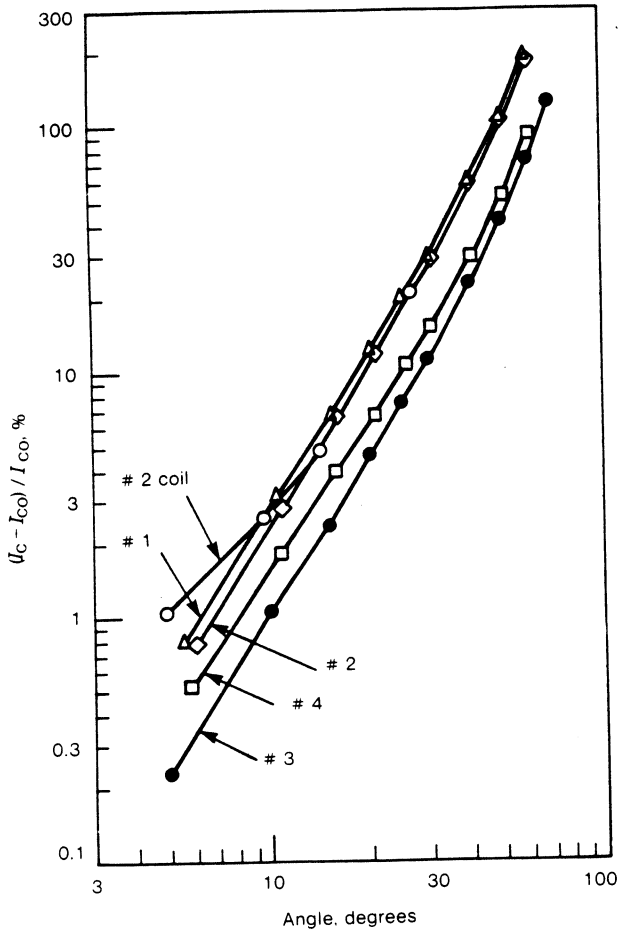

Fig. 13 Full log plot of data shown on Fig. 12, including some larger angle data. I_{co} is the critical current at the zero angle

to currents less than about 400 A, but higher field data on the twisted multifilamentary Nb_3Sn sample and sample 2 indicated that the curves on Fig. 13 can be extrapolated to 90°.

The effect of field orientation with respect to the faces of the rectangular conductors was investigated using a long straight sample in the radial-access magnet. The field is always normal to the conductor axis in these tests. The results are shown in Fig. 14 where I_{co} is the critical current with the field parallel to the wide face of the conductor. Measurements at 3 and 7 T (7 T data shown in Fig. 14) indicated that $(I_c - I_{co})/I_{co}$ was a good magnetic field scaling of this effect. There are several interesting features here. The most important from the standpoint of experimental design is that moderate care in positioning the sample will result in good data when the measurement configuration has the field parallel to the wide face. This configuration is the one most commonly encountered in the high field region of simple magnet windings. On the other hand, the configuration that has the field normal to the wide face has a stronger angular dependence for the critical current and, thus, measurements in this position will require significantly more care in sample orientation. The figure shows another interesting effect in that the angular dependence of the critical current of the tape conductor is opposite to that of the rectangular multifilamentary conductor. This is probably due to a difference in the pinning mechanism of these two types of superconductors. This topic of aspect ratio and its effect on I_c is a very interesting one and is currently under study at NBS.

Strain. Proper assessment of the sources and effects of strain on the sample is one of the most critical aspects of experimental design. The problem is complicated because sample strain may arise from many sources including: differential thermal contraction of the apparatus, both static and dynamic (due to different cooling rates); sample mounting; and Lorentz force. In addition, the complex nature of the composite conductor makes detailed evaluation of the strain in the twisted filaments quite difficult. A recent comprehensive review of this topic has been published by Ekin[8] and should be consulted for details on the effects of strain within the superconducting composite.

An important feature of strain effects is the extreme difference between NbTi and Nb_3Sn. Niobium-titanium conductors are generally very strain tolerant. Their critical current is not degraded significantly (1%) until the overall tensile strain reaches ~0.5%. Further straining to 2% gives only a 10% degradation of I_c.[8] Niobium-tin, on the other hand, is very sensitive to strain as illustrated by Fig. 15 from the review just mentioned. The intrinsic strain is that existing in the Nb_3Sn itself and may have components from the conductor matrix material. Thus, a particular sample may

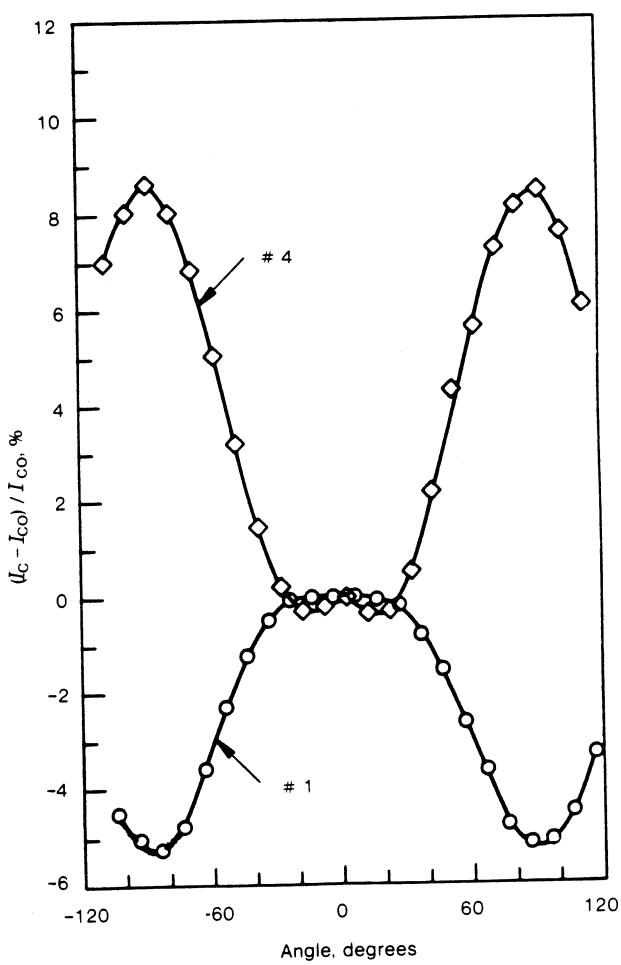

Fig. 14 Dependence of I_c on rotational angle of field around the conductor axis for rectangular conductors at 7 T. The zero angle is defined where the field is parallel to the wide face of the conductor and I_{co} is the critical current at the zero angle

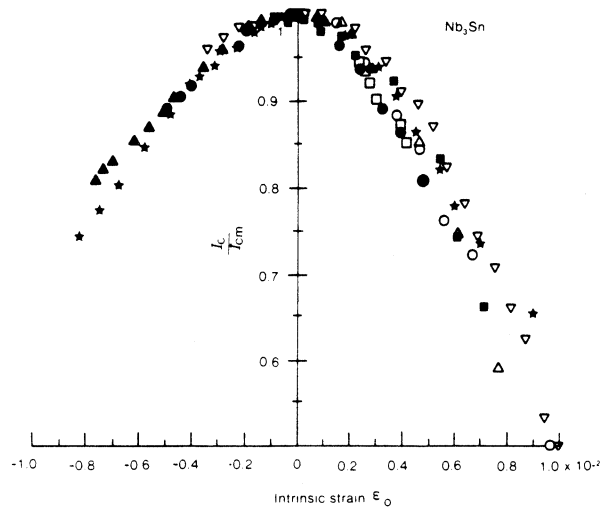

Fig. 15 Effect of intrinsic strain on the critical current of commercial multifilamentary Nb_3Sn. From reference 8, I_{cm} is the maximum critical current

lie on either side of the peak when under no external stress. In any event, it is clear that strains as small as 0.2% may result in significant changes in I_c. One practical result is that samples of Nb_3Sn conductor must usually be formed to the shape required for the test before they are given the final reaction heat treatment to form the intermetallic compound (to avoid introducing bending strain).

Another aspect of the strain dependence of critical current that is important for measurements and applications near the upper critical field is that the strain dependence becomes a strong function of magnetic field. This occurs for both NbTi and Nb_3Sn, but is probably only significant at reasonable strain values for the latter. Data illustrating this effect is shown in Fig. 16 from recent measurements by Ekin.[9] Recent theoretical and experimental work[9,10] has led to a mathematical description of this strain-scaling behaviour and these papers should be consulted if measurements at high fields (above about 10 T) are contemplated.

Strains induced by differential thermal contraction of the sample holder with respect to the sample may be large because the holder is most often a nonmetallic substance and these materials contract much more on cooling than metals. The two most common solutions are to make a metallic sample holder or to use a nonmetallic composite, usually epoxy-fibreglass. The former approach is not recommended because of the problems associated with electrical insulation. The fibreglass-epoxy materials, especially NEMA G-10, are useful if proper attention is paid to the large thermal expansion anisotropy. Typical data taken in our laboratory[11] are shown in Fig. 17 for both G10 and G11 fibreglass-epoxy as well as the much less expensive (and less well characterized) cotton phenolic. Data are also given in the reference for both NbTi and Nb_3Sn commercial multifilamentary conductors. They fall within the range of the "warp direction" curves. Thus, for example, the best way to make the bottom segment of a round-bottom hairpin is by using a piece of rolled cloth fibreglass-epoxy tube with its axis normal to the centreline of the apparatus.

Attachment of bus bars and such to these nonmetallic holders is easily accomplished with filled epoxies that also match the thermal expansion reasonably well. Both the fibreglass-epoxy and the filled epoxies can withstand the heating required for making soft solder joints. An insulating electrical varnish soluble in alcohol-toluene is used for holding down voltage leads and other low stress, non-permanent applications.

The Lorentz force is a serious source of strain because of the high currents and fields involved in critical current testing. The force on a conductor carrying 600 A in a 10 T field is 60 kg per centimetre of length. Also, because of the form of the dependence of I_c on H, this force reaches its maximum at relatively low fields for practical conductors. The problem is usually solved by laying the test sample in a fairly tight-fitting groove in the holder and orienting the sample with respect to the field so that the force is directed into the holder. There are experiments, such as rotation tests in the long straight geometry, where this solution cannot be used. In that case either a special holder is needed or one must use varnish or grease to hold the sample in place and the contraction precautions observed. This solution also has the potential of restricting the transfer of heat from the sample to the bath resulting in the self-heating effects described below.

Temperature. There are numerous ways by which heat can be introduced into the test specimen. Some of them have already been mentioned, such as contact heating, heating due to current transfer between filaments, and the intrinsic heating that occurs near I_c. In addition, rapidly varying the sample current or the magnetic field can introduce eddy current heating. The specific heat of all common materials

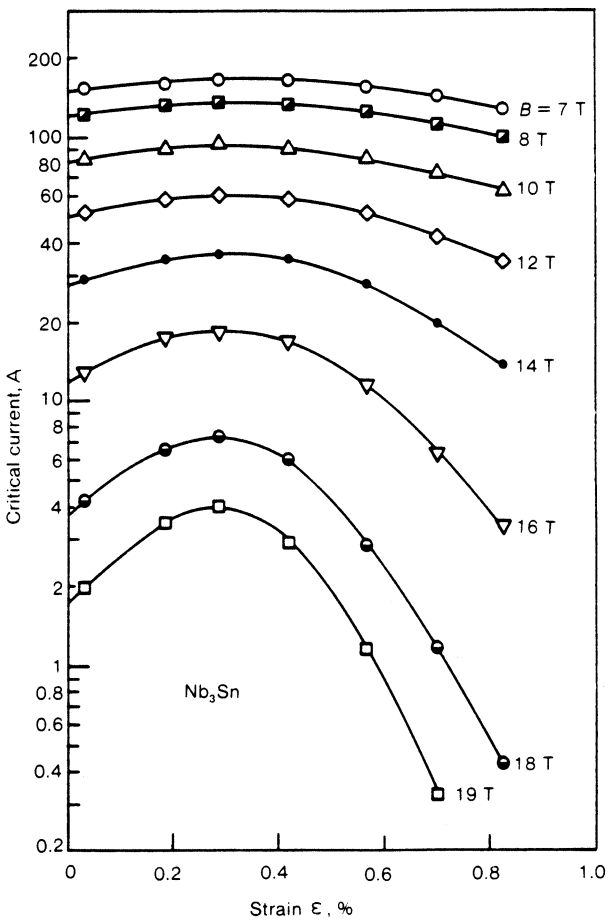

Fig. 16 Observed change in the effect of strain on the critical current of Nb_3Sn conductor at fields near the upper critical field. From reference 9

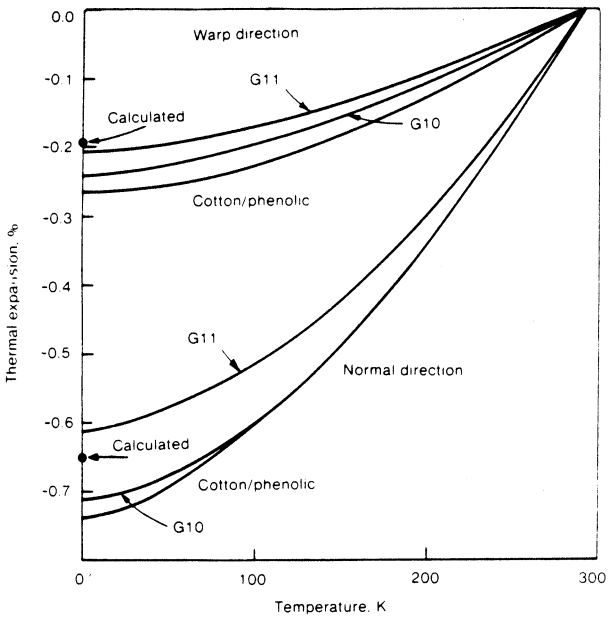

Fig. 17 Thermal contraction of nonmetallics used in sample holder construction. From reference 11

is extremely low at liquid helium temperature and, thus, a small energy input can result in a large temperature excursion. The use of varnish and/or grease on the test sample for mechanical stability may result in lowered thermal stability as mentioned above. Reasonable care in making joints is generally all that is required for preventing thermal runaway.

There is a more subtle thermal effect that is more common. In this case, the *V-I* data are still normal in appearance and behaviour, but the value of I_c is reduced by 1-4% depending on the criterion used (greatest reduction for high criteria) and on the magnetic field (greatest reduction for lower fields). Detection of this situation requires careful examination of the *V-I* curve in the flux flow region. As we will see shortly, the voltage there is approximately proportional to I^n. Values of n cover a wide range in general, but for a given material n is reasonably constant. When the heating effect occurs, the value of n changes dramatically, because I_c is a function of temperature, which in turn is a function of where the sample is on the *V-I* curve. A typical example from our Nb_3Sn data: $n = 23$ for a normal run, but for a run with a relatively light coat of grease on the wire $n \geq 30$ at the higher electric fields (within a factor of five of quench). A practical technique for avoiding this problem is to determine the sample voltage at quench and use a criterion that is well below that (factor of five or ten).

Experiment execution and data analysis

The successful execution of a critical current measurement requires consideration of a number of points that do not exist in conventional resistivity work. Not the least of these is the definition of critical current. This is not a philosophical question, but rather a practical one involving the choice of an appropriate criterion of electric field or resistivity. Similarly the voltage caused by currents travelling through the non-superconducting currents matrix must be treated with care in the data analysis. These problems and numerous other, more mundane ones are the subject of this section.

V-I curve measurement. The sample voltmeter shown in Fig. 5 may be either digital or analogue. We have used both. The analogue meter is a commercial nonovoltmeter. If a battery power supply is used for sample current, the noise level is down to ~2 nV and this combination provides the greatest sensitivity. However, when an SCR regulated power supply is used, the SCR switching noise reduces the sensitivity of the nanovoltmeter to ~100 nV. In this case it offers no advantage over the digital voltmeter. Our measurements of I_c using the two meters (with the SCR current supply) agreed to within 0.5%.

The choice of a criterion to define the point on the *V-I* curve where the critical current is reached is most often determined by the potential application of the conductor. Large, high field conductors may use relatively high criteria, while conductors for NMR magnets may require very low values.

The criterion may be stated in terms of either electric field or resistivity. The electric field criterion indicates the voltage drop per unit length of the superconductor in the flux-flow state at the critical current. Typical values range from 0.1 to 10 $\mu V\ cm^{-1}$ for conductors with critical currents of less than 600 A. The resistivity criterion refers to the effective resistivity of the superconductor in the flux-flow state, ie, the voltage drop per unit length divided by the current per unit area. Typical values for the resistivity criterion range from 10^{-12} to $10^{-10}\ \Omega$ cm using the total cross-sectional area of the conductor. One problem with the resistivity criterion is deciding what cross-sectional area to use to calculate the resistivity. The case of a NbTi conductor is fairly simple, either the total area of the conductor, or that of the NbTi alone is used. For a Nb_3Sn conductor the area used may be: the total area of the conductor; the non-copper area (which may include the area of the diffusion barrier, bronze, Nb, and Nb_3Sn); the area of the Nb and Nb_3Sn; or the area of the Nb_3Sn alone. The determination of some of these areas involves extensive metallography and statistical techniques, which means it is difficult and very time consuming. For our multifilamentary Nb_3Sn superconductor, the total cross-sectional area is about fourteen times that of just the Nb and Nb_3Sn. The critical current values determined at 7 T using a resistivity criterion of $10^{-11}\ \Omega$ cm and these two areas differ by about 19%.

We choose to use the electric field criterion. It does not penalize highly stabilized conductors and it can easily be converted into an equivalent resistivity criterion using the total cross-sectional area of the conductor. One should note that a given electric field criterion does not correspond to the same resistivity criterion at all values of magnetic field. At high fields a given E_c corresponds to a larger value of resistivity than at low fields. This could be a problem very near to the upper critical field, H_{c2} (because every conductor will show a finite critical current for any value of E_c), but most practical applications are restricted to upper fields of 0.8 H_{c2} or less.

The effect of choice of criterion on the value measured for the critical current is shown in Fig. 18 for NbTi and in Fig. 19 for Nb_3Sn. These plots illustrate how I_c scales with criteria and magnetic field where I_{c0} is the critical current at 0.1 $\mu V\ cm^{-1}$ for NbTi and 1 $\mu V\ cm^{-1}$ for Nb_3Sn. The irregular shape of the curves at the lower criteria reflect the uncertainty of those values. These data were taken using a coil sample in order to minimize the current transfer voltages that must be subtracted out at the lower criteria. Clearly, there is a systematic variation with criterion as one

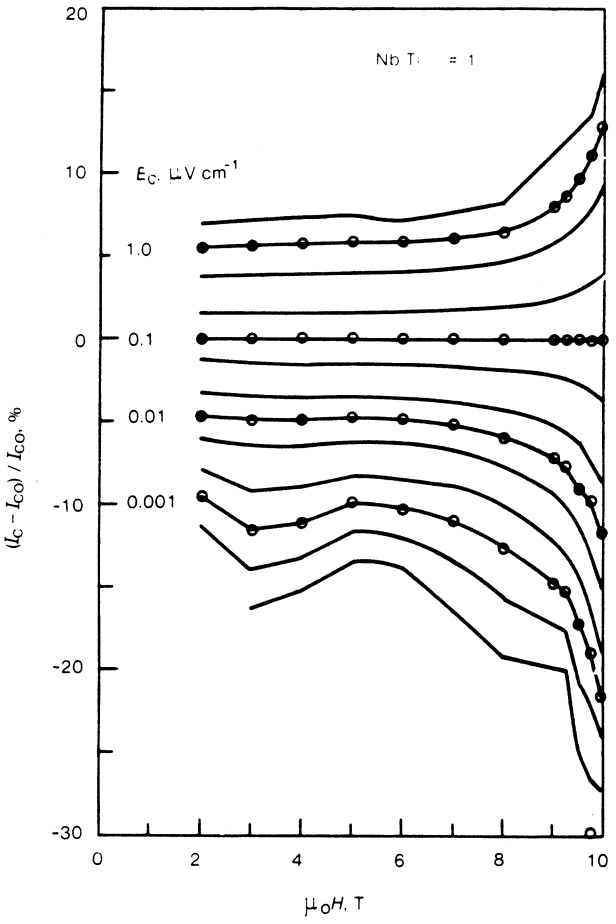

Fig. 18 Dependence of the critical current of NbTi conductor (# 1) on magnetic field for various electric field criteria (1, 2, 5 sequence). The vertical axis is normalized to I_c at 0.1 μV cm^{-1}, I_{co}

would expect from the shape of the *V-I* curve. For both conductors there is only a slight dependence on field for values likely to be encountered in a reasonable test (use of NbTi at fields >8 T is not common at 4 K, nor is the use of criteria <10 nV cm^{-1}).

The behaviour shown in the figures is another manifestation of the power law dependence

$$E \alpha I^n \qquad (2)$$

in the flux flow region that was mentioned earlier. The sharper the transition (large *n*), the smaller the effect of choice of criterion on the critical current value obtained. Evaluation of *n* is not a critical part of a normal experiment, but knowledge of its expected behaviour is helpful in analyzing problems, such as sample heating. In addition, a well-characterized *n* of a particular sample could be used to extrapolate to a lower criterion than can be achieved in another measurement. Selected data from our samples are given in Table 4. Very similar values of *n* will be obtained if one uses critical current data based on a resistivity criteria. The NbTi data (sample #1) are plotted in Fig. 20. The uncertainty in the value of I_c at the lower criteria cause the irregular shape of *n* calculated using those values. The conclusion to be drawn here is that each material has a value of *n* associated with it that depends somewhat on the criterion chosen and on the magnetic field. The value decreases, usually slightly, with increasing field. Values of *n* generally lie between 20 and 100. Variations of 10 to 20% in the value of *n* do not reflect significant change in the shape of the *V-I* curve. Significantly higher or lower ones nearly always indicate a problem in the measurement.

Current. The usual measurement technique involves establishing a constant magnetic field and ramping the sample current to trace out the *V-I* curve. Generally the ramp rate chosen is relatively slow (a few minutes to I_c), but even under these conditions voltages may be induced in the leads to the sample voltage taps during sensitive measurements. The technique for evaluating the magnitude of this effect is to stop part way up the *V-I* curve and start the current decreasing at the same rate for a few amperes. The (usually small) loop traced out measures the dI/dt signal. The effect can be minimized by carefully twisting all voltage lead pairs and providing minimum area at the sample itself. This latter consideration is especially important in the inductive coil geometry, where the voltage leads should be co-wound with the sample.

Ripple or SCR spikes on the current supply can make measurements at very low criteria impossible, as we discussed in the last section. At more reasonable criteria, however, these disturbances have no significant effect on

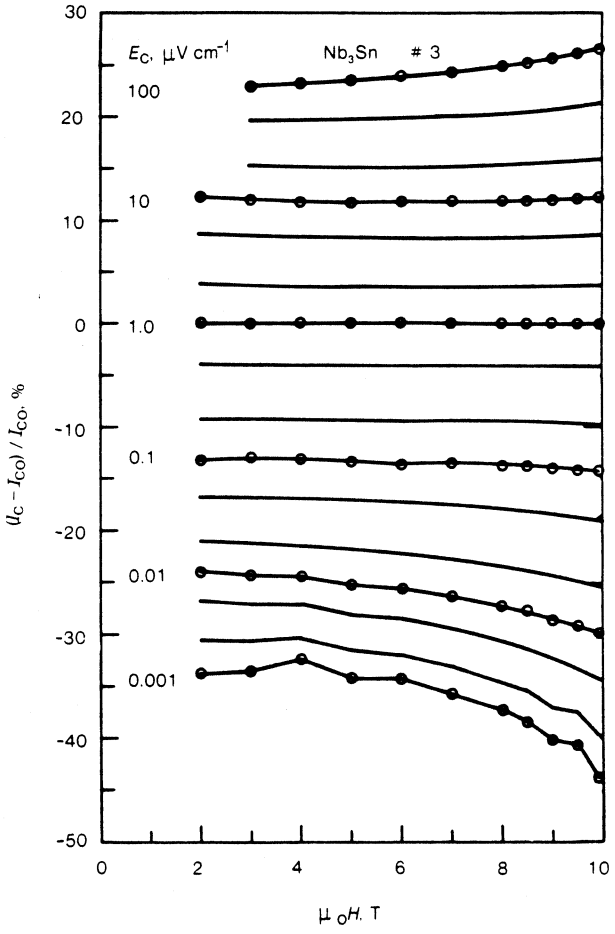

Fig. 19 Dependence of the critical current of Nb_3Sn conductor (# 3) on magnetic field for various electric field criteria (1, 2, 5 sequence). The vertical axis is normalized to I_c at 1.0 μV cm^{-1}, I_{co}

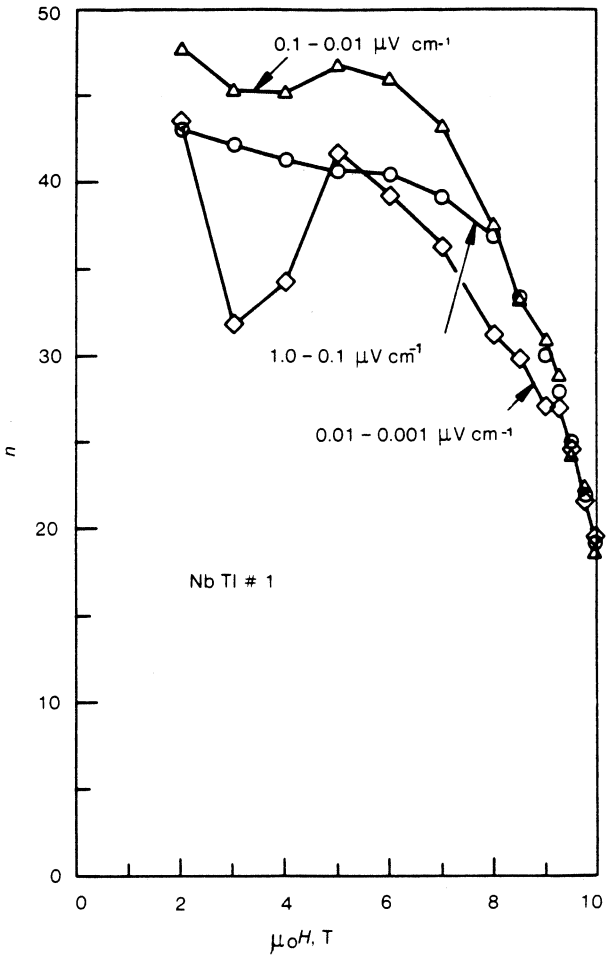

Fig. 20 Behaviour of the exponent, n, as a function of magnetic field for various ranges of the electric field criterion. The sample is NbTi (# 1) in a coil configuration

the results, as shown in Fig. 21, which compares data taken with a zero-ripple battery supply to those with a commercial 600 A SCR supply. The agreement between these two was within the precision of the measurement (± 0.2%) except for the Nb_3Sn tape sample. The Nb_3Sn tape was expected to be the worst case in this comparison because of the higher ac loss of this type of sample and it may be showing this effect, but it was only 0.5% at 7 T.

Magnetic field. There are sources of extraneous signals related to time variation of the magnetic field such as ripple and drift of the magnet supply. These are rarely a serious problem in a conventional measurement. The prescription for minimizing them is, as above, to create a minimum loop area in the various leads. Coil samples offer the greatest potential for problems here and, for very precise work, a noninductively wound sample may be required.

Because of the shape of the curve of critical current vs magnetic field for practical conductors, small errors in field measurement can result in relatively large errors in the critical current. The dependence of I_c (E_c = 0.1 μV cm^{-1}) on magnetic field for our test samples is illustrated in Fig. 22. In preparation for a series of measurements, the field and field profile of the magnet should be measured. The field should be known to ± 1% and should not vary by more than that over the measurement region of the sample, ie, between the voltage taps.

The concept of self field is often mentioned. This field is the one that is produced by the sample current. Fig. 23 illustrates the self-field effect on a representative row (a–e) of twisted filaments in a conductor. Suppose that, if the filaments were not twisted, these five filaments could carry a total of 100 A (16, 18, 20, 22, and 24 A) with a flux-flow electric field of 1 μV cm^{-1}. If the filaments are twisted the critical current of each twisted filament will depend on its position relative to the magnetic field profile (greatly exaggerated to show this effect). Then current above 88 A will have to transfer through the normal matrix to redistribute among the filaments and an additional electric field will result depending on the twist length and current transfer characteristics of the conductor. The additional current transfer voltage will cause a reduction in the critical current for a given criterion, ie, the total electric field will reach 1 μV cm^{-1} at a current less than 100 A. This is analogous to the bending strain effect where the spatial strain causes a spatially dependent current density. In conductors of the size considered here, the magnitude of the self-field effect is small. Furthermore, the effect is similar in both the I_c measurement and in most applications. In very large conductors made up of cabled and/or fully transposed strands in various cross-sectional shapes, the effect could be important when attempting to predict the behaviour from that of a single strand.

Temperature. The effect of bath temperature on the critical current is one of the least well appreciated aspects of this

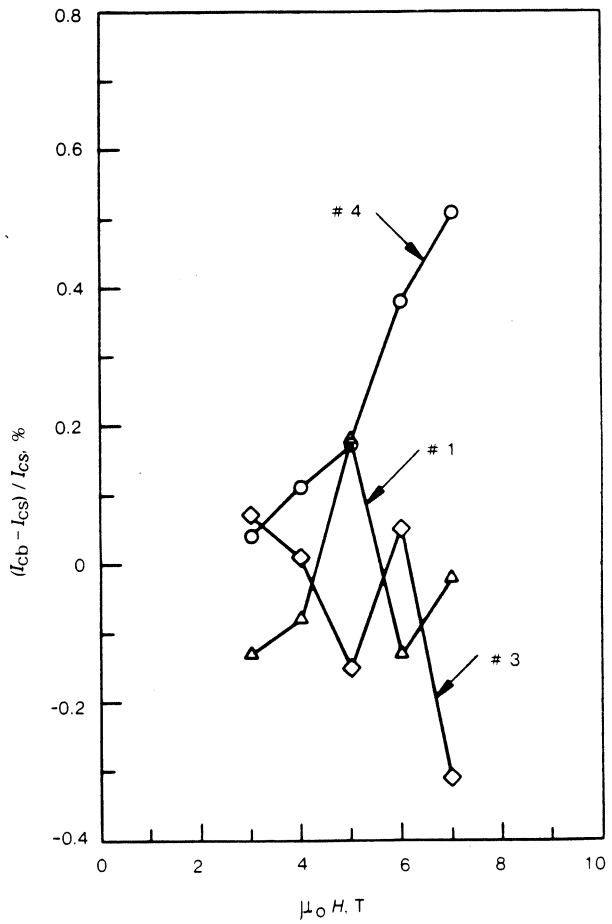

Fig. 21 Relative critical current values determined using a battery power supply (I_{cb}) and an SCR regulated one (I_{cs}). Samples are identified in Table 1

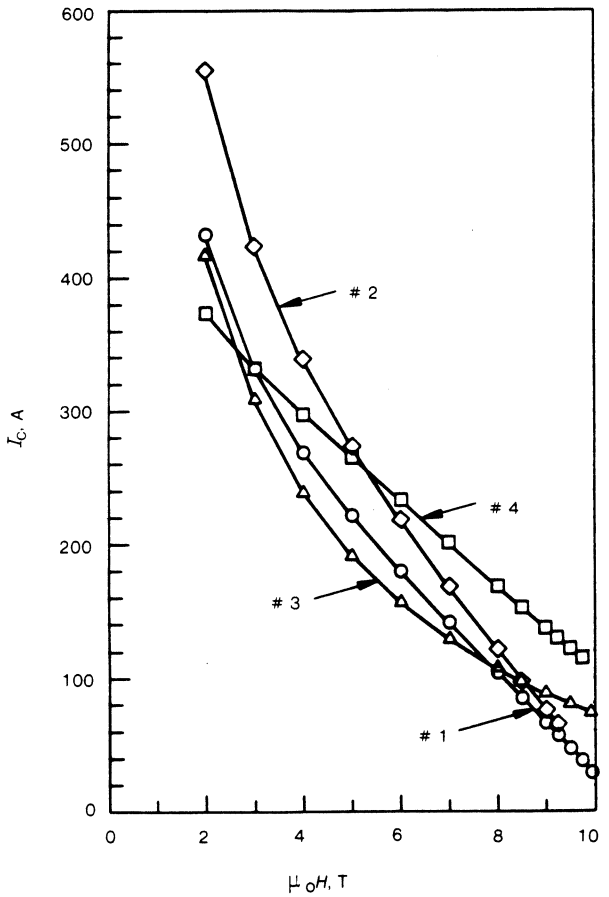

Fig. 22 Magnetic field dependence of the critical current for the samples of Table 1

type of measurement. It is our contention that a meaningful report of I_c data for commercial use requires a statement of the sample temperature to ± 0.5%. Usually the assumption is made that the sample temperature is that of the bath and, in most cases, that seems to be adequate. The temperature of the liquid helium depends on the ambient pressure. The small additional pressure in the dewar caused by hydrostatic pressure and the use of vapour-cooled current leads is not usually significant ($\lesssim$ 10 mK) but could become so if the leads are partially blocked. Typical atmospheric pressure variations over the course of a year (typhoons, hurricanes, and tornados excluded) translate to bath temperature variations of about ±20 mK. To avoid problems it is recommended that the pressure in the dewar be monitored during the measurement. The bath temperature can then be determined from standard tables.[12]

Some justification is required for the above "hard line" on this subject. Extensive data have recently been presented on both NbTi and Nb_3Sn by two groups.[13,14] The basic result of these papers is that the critical current is observed to be related to the temperature by

$$I_c \alpha (T_c^* - T) \qquad (3)$$

where T_c^* is the bulk critical temperature at a given field. T_c^* is usually determined by extrapolating $I_c(T)$ (for temperatures near the temperature of interest) to zero. The intercept is defined as T_c^*. At high fields, the value of T_c^* can be quite low. Data on multifilamentary wires of NbTi give T_c^* = 5.4 K at 8 T[13] and 8.4 K for multifilamentary Nb_3Sn at 12 T.[14] Especially at high fields, the variation in bath temperature from day to day can be a significant fraction of the quantity $T_c^* - T$ and thus have a large effect on the I_c measurement.

Another temperature-related consideration is the minimization of thermoelectric voltages that occur because of the large temperature gradients encountered by the voltage leads in a typical experiment. These voltages can be greatly reduced by proper thermal anchoring of the leads in the region of the sample[15] and by the use of continuous copper wires from the sample to the voltmeter input. This involves making feedthroughs for the top plate of the cryostat. Using this technique, the thermoelectric voltages can be reduced to the order of several tens of nanovolts and, more importantly, they tend to remain constant over the time required to make a measurement.

Current transfer. This topic has been mentioned several times already. It can be a problem in even the best designed experiment in that it introduces current-dependent voltages of significant size. Frequently one has no choice but to try to remove these extraneous signals during the data analysis. The voltages arise because current flows through the normal metal stabilizer of the superconductor in the process of attaining an equilibrium distribution. The situations that lead to this current flow may result from a number of causes. Current entering the sample from the bus bar is a

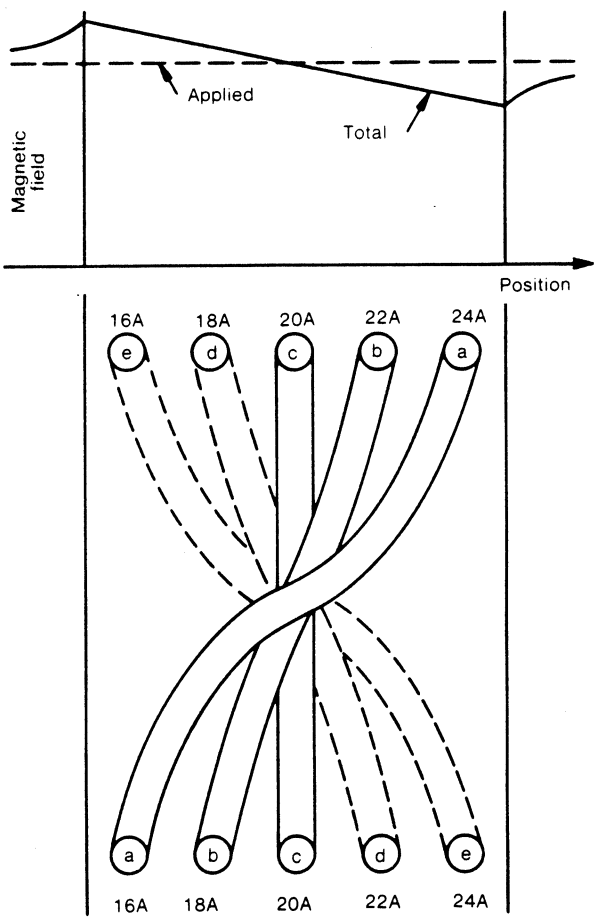

Fig. 23 Schematic of self-field effect showing a representative row of twisted filaments in a conductor, their critical currents and exaggerated field profile

Table 5. Tolerance for critical current variables

Variable	Suggested uncertainty, %	Resultant ΔI_c, %
I	1	1
I, ripple	5	1
E_c	12 (10% I, 6% V)	1
H	1	2.5
H, ripple	1	0.5
H, uniformity	2	1.5
H, angle	7°	1
T	0.5	1
ϵ, bending	0.1 Nb_3Sn 2 NbTi	2
ϵ, tensile	0.05 Nb_3Sn 0.5 NbTi	2

major source of transfer voltage (such as that encountered in the short geometry) as illustrated for the low current parts of the V-I curves in Fig. 8. In addition, transit through a region of field gradient (such as that encountered in the long geometry) or, similarly, a change in the direction of the current path with respect to the field (such as that encountered in the hairpin geometry) will cause current redistribution regardless of the length of the sample in the low or parallel field region. The situation is further complicated by the twist of the superconducting filaments that may result in negative current transfer voltages, ie, the transferring current is apparently flowing against the voltage gradient. While all this has been explained in the references previously listed, it is another matter to properly handle data that contain these voltages.

Simply put, the data analysis problem is to subtract off the current transfer voltage so that the chosen electric field criterion can be applied to the intrinsic V-I curve. When the current transfer voltage is a small fraction of the total signal at I_c, there is clearly no problem. Also, for relatively insensitive measurements, such as are often encountered in routine testing, the current transfer voltage can usually be approximated by a straight line at low current and thus easily extrapolated out to the I_c region. In other cases where the voltage is not linear with current and is of significant size, a reasonable approach is to plot log V versus log I similar to Fig. 8 which should result in a break in slope between the current-transfer region and the intrinsic flux-flow region. The lower current transfer portion can then be approximated by a straight line (power law) and subtracted from the data. This was done for the data presented here and the slope of log V versus log I in the current transfer region was as high as 2 to 3. If a large number of samples are involved, this technique may not be feasible and a change in experimental design is suggested. In any case, however, when the current transfer voltage is large compared to the criterion, it is easy to over or underestimate the current transfer contribution and get erroneous results. This is illustrated by the variation in I_c shown in Table 3 for the different sample holders (see Fig. 8 also). If very precise data are required it is best to go to a coil sample.

Summary

The data and discussion presented in the previous sections should allow one to construct an apparatus and carry out a successful critical current measurement. Clearly, several levels of sophistication can be achieved and the choice is really one of money, time, and needs. Table 5 provides a summary of the suggested accuracies for the various parameters and their effect on the final measurement. In some cases (eg, uniformity and angle of H) these figures assume that the conditions are not at the extreme limit for the total length of the sample between the voltage taps. The resulting error from all sources listed is $< 5\%$.

We should re-emphasize that the work presented here is for relatively small conductors with $I_c < 600$ A. The very large conductors now available present a few additional problems that have not been addressed such as complicated strain configurations, internal motion, large self fields, and probably complex voltage patterns in the flux flow region. In any event, the average laboratory is not equipped to handle conductors of this size and those few that are, should be well aware of the problems.

There are two further developments that we feel would contribute greatly to the critical current measurement. A more thorough understanding of stability in practical composites and the availability of a standard multifilamentary superconductor for evaluating new apparatus and maintaining the accuracy of frequently used systems. Both of these topics are now being investigated at NBS.

The help and support of the remainder of the Group at NBS, especially A.F. Clark and J.W. Ekin are gratefully acknowledged. The ASTM committee B01.08 on Superconductors has provided guidance and served as a sounding board for many of the ideas presented here. The support and interest of D. Sutter and D. Beard of DoE and P. Marston of MIT made this work possible. Ms. V. Grove once again made production of the finished manuscript a painless operation.

References

1 **Fickett, F.R., Clark, A.F.,** Development of standards for superconductors, annual report FY79, NBSIR 80-1629 (December 1979)
2 **Fickett, F.R., Goodrich, L.F., Clark, A.F.,** Development of standards for superconductors, annual report FY80, NBSIR 80-1642 (December 1980)
3 **Brechna, H.,** Superconducting magnet systems Springer-Verlag, New York, (1973)
4 **Scott, R.B.,** Cryogenic engineering, D. Van Nostrand, New York, (1959)
5 **Goodrich, L.F., Ekin, J.W.,** Lap joint resistance and intrinsic critical current measurements on a NbTi superconducting wire, *IEEE Trans Mag* **MAG-17,** (1981) 69
6 **Goodrich, L.F., Ekin, J.W., Fickett, F.R.,** Effect of twist pitch on short-sample V-I characteristics of multifilamentary superconductors, Advances in cryogenic engineering - materials **28** (to be published)
7 **Ekin, J.W.,** Current transfer in multifilamentary superconductors, I. Theory, *J Appl Phys* **49** (1978) 3406
8 **Ekin, J.W.,** Mechanical and properties and strain effects in superconductors, Superconductor materials science: metallurgy, fabrication, and applications, (ed) S. Foner, B.B. Schwartz Plenum Press, New York, (1981) 455
9 **Ekin, J.W.,** Strain scaling law for flux pinning in practical superconductors. Part 1: basic relationship and application to Nb_3Sn conductors *Cryogenics* **20** (1980) 611
10 **Ekin, J.W.,** Strain scaling law for flux pinning in practical superconductors, Part 2: Application to NbTi, V_3Ga,

Nb_3Ge, Nb_3Al, and Nb-Sn based ternary superconductors *Cryogenics* **22** (1982) to be published
11 **Clark, A.F., Fujii, G., Ranney, M.A.,** The thermal expansion of several materials for superconducting magnets, *IEEE Trans Mag* **MAG-17** (1981) 2316
12 **McCarty, R.D.,** Thermophysical properties of helium-4 from 2 to 1500 K with pressures to 1000 atmospheres, *NBS Technical Note 631* November (1972)
13 **Spencer, C.R., Sanger, P.A., Young, M.,** The temperature and magnetic field dependence of superconducting critical current densities of multifilamentary Nb_3Sn and NbTi composite wires, *IEEE Trans on Mag* **MAG-15** (1979) 76
14 **Schauer, W., Zimmerman, F.,** Temperature dependence of the critical current and pinning behaviour for Nb_3Sn filamentary superconductors, Adv Cry Eng **26** (1980) 432
15 **Hust, J.G.,** Thermal anchoring of wires in cryogenic apparatus, Rev *Sci Instr* **41** (1970) 622

Superconductor technology from IGC

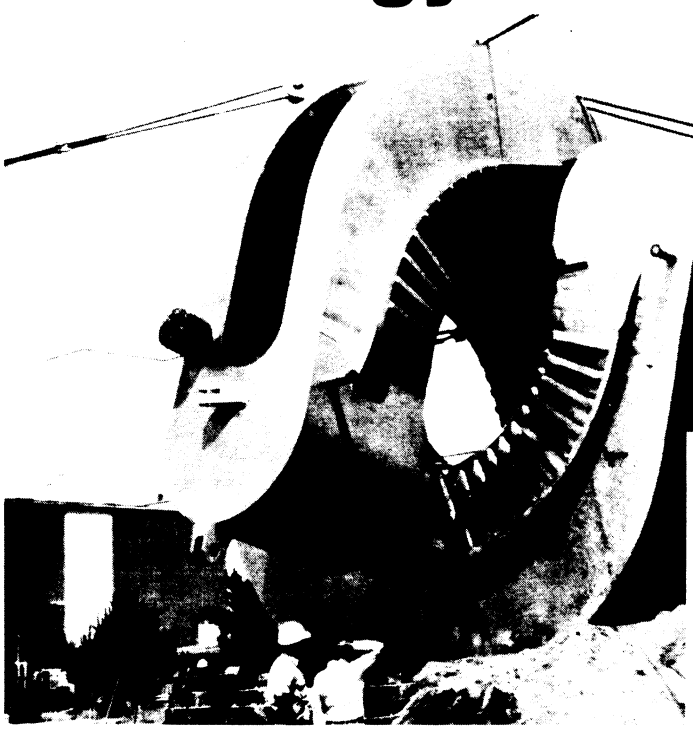

Photo Courtesy of Lawrence Livermore National Laboratory.

Mirror Fusion Magnet at Lawrence Livermore National Laboratory uses IGC Superconductor.

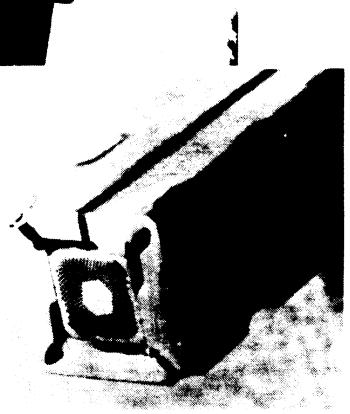

Superconductive Monolith after Cladding with Convoluted Copper Wrap for the MFTF Magnets.

Intermagnetics General Corporation (IGC) is one of the world's leading suppliers of NbTi superconductor and related magnet design technology for fusion magnets, MHD magnets and high energy physics applications.

In addition to superconductor for the LLNL Mirror Fusion Test Facility (6.5mm Square Monolith - 11,000 Amps at 7.5 Tesla), shown above, we are supplying superconductor for many other large scale applications including:

- **ORNL Large Coil Program**
  (Cryostable Cable - 13,000 Amps at 8 Tesla)
- **Fermilab Energy Doubler/Saver Accelerator**
  (23 Strand Cable - 5,000 Amps at 5 Tesla)
- **CDIF Giant MHD Saddle Magnet**
  (NbTi Strands Cabled over a Stabilizing Core - 6,000 Amps at 7 Tesla)

IGC supplies a wide range of NbTi and Nb_3Sn superconductors for most applications. For more information contact John Scudiere, Sales Manager — IGC Conductor Division.

IGC INTERMAGNETICS GENERAL CORPORATION

Charles Industrial Park, New Karner Road, Guilderland, NY 12084
Telephone: (518) 456-5456, TWX: 710 441-8238